DOI 10.1007/s10812-019-00816-2
Journal of Applied Spectroscopy, Vol. 86, No. 2, May, 2019 (Russian Original Vol. 86, No. 2, March–April, 2019)

RAMAN SPECTROSCOPIC INVESTIGATION OF OLEFINS IN SATURATED HYDROCARBONS AND SELF-TUNING MODEL DEVELOPMENT

A. Kh. Kuptsov,*[*] O. G. Karchevskaya, T. E. Kron,
G. A. Korneeva, and E. V. Zhmaeva

UDC 53.083;665.658;665.612.2;54.057

Based on systematized collection of Raman spectra of about 40 monounsaturated olefins, spectral patterns and invariant relations were established that formed the basis of the method for determining total olefins (total unsaturation per 100 carbon atoms) and their main classes in solutions of saturated hydrocarbons. Self-tuning of the model by calculating the proportion of spectrally unresolvable C=C components using the intensity of conjugated methyl groups increased its accuracy. In terms of repeatability, speed and cost-effectiveness of the analysis, the Raman-method is superior to standard methods of gas and adsorption chromatography and other modern spectral-correlation methods. The accuracy and stability of the results repeatability is confirmed by more than annual series of parallel comparisons with the data of known method. It is shown that five types of olefins in paraffin model solutions are sufficient to construct calibration curves in units of the number of C=C bonds per 100 carbon atoms. These units make it possible to transform the data to the iodine scale and unify the calibration model for different fractions regardless of the hydrocarbon chain length. The Raman technique can be extended to analyze other mixtures of non-aromatic hydrocarbons and be used for remote control of processes via fiber optic cables in industrial production.

Keywords: *Raman spectroscopy, olefins, self-tuning model, process control.*

Introduction. Modern spectral methods with fiber-optic radiation input for monitoring processes involving hydrocarbons provide technical and economic advantages over traditional methods both in laboratory conditions and in industrial production, as shown in [1, 2], in particular, using Raman spectroscopy [3, 4]. Investment recovery in monitoring technologies occurs due to, firstly, the exclusion of defects, the speed, accuracy and stability of quality indicators determination, management efficiency improvement, and process optimization; secondly, industrial control cost reduction; thirdly, conversion of some of the expenses for standard analytical control into additional capitalization of processes by creating new technical solutions and patents for control methods.

Control of the most common in tonnage processes that involve reactions on C=C bonds is particularly of interest. One of the richest sources of olefins can be "synthetic oil" obtained by the conversion of methane and other light gases by the Fischer–Tropsch process [5]. Molecular spectroscopy methods widely used in hydrocarbon studies — UV-Vis-IR absorption, fluorescence, Raman — are promising for industrial process control due to the high content of information they provide, their efficiency, and analysis speed compared to many traditional physicochemical and chromatographic methods, especially when express determination of total structural group characteristics is required. The possibility of remotely controlling a number of product streams by a single spectrometer through networks of special optical fibers makes them more attractive than mass spectrometry and NMR methods. Spectroscopy of composite bands and overtone bands in the near-infrared range is most widely used for real-time analysis through optical fibers. Undoubtedly, the advantages of these methods over traditional mid-IR spectroscopy of the fundamental vibrations are higher optical fiber opacity length (hundreds of meters as opposed to just a few), superior wear resistance of glass optical windows compared to hygroscopic salt windows, rheological advantages of flow-through cells with a thick optical layer (2–12 mm) compared with a thin optical layer (0.02–0.50 mm), explosion

---

[*] To whom correspondence should be addressed.

LLC "United R&D Centre," 55/1, Bld. 2, Leninsky Ave., Moscow, 119333, Russia; email: KuptsovAK@rn-rdc.ru.
Translated from Zhurnal Prikladnoi Spektroskopii, Vol. 86, No. 2, pp. 290–297, March–April, 2019. Original article submitted December 3, 2018.

safety in the production atmosphere of halogen lamps compared to hot ceramic sources. The relatively lower information content of the near-IR range is compensated using multivariate chemometric data processing methods (although chemometric models are also used for Raman spectral prediction, for example, of gasoline properties [6–9]). The main contributor to the initial accuracy of the model is the accuracy of the reference method. The disadvantage of correlation models based on the reference data of standard methods is the limitation of their applicability to a range of samples and measurement conditions, the variation limits of which are set when training a model. The variability of the composition of hydrocarbons and the wide temperature fluctuations of product flows lead to degradation of the quality of correlation models as they are used at industrial sites. This makes the development of a direct Raman spectroscopy method for analyzing olefin-containing hydrocarbons appropriate for more reliable and accurate quantitative rapid determination of the degree of unsaturation in monitoring the processes of synthesis, hydrogenation, hydroformylation, etc.

In the present work, various methods of Fourier transform IR (FTIR) (transmission and attenuated total reflection (ATR) using the Avatar Multi-Bounce HATR accessory) and Fourier transform Raman (FT Raman) spectroscopy are used to investigate 11 batches of samples of synthetic liquid hydrocarbons obtained by the Fischer–Tropsch process (SLH FT), products of their hydrogenation and hydroformylation, and other hydrocarbons containing olefins. The homologous series of C6–C12 α-olefins and olefins with *cis*- and *trans*-unsaturation in 2-, 3-, 4-positions, tri- and tetrasubstituted olefins, series of their calibration solutions in paraffins with different numbers of carbon atoms prepared by the gravimetric method were studied. In addition to studying the spectra of prepared samples, a computational analysis was conducted of the previously obtained digital FTIR and FT Raman spectra of *cis*-, *trans*-polyoctenamers, monomers of classes 1.1.1 and 1.1.2 and low molecular weight compounds of class 4.4 from the digital collection of vibrational spectra [10–12]. Paraffins and isoparaffins, as well as fully hydrogenated SLH FT, were used as solvents.

Experiment. Raman spectra were recorded using a Nexus FT Raman spectrometer (Thermo-Nicolet, USA) using a 180^o scattering angle with excitation by YVO_4:Nd laser radiation at λ = 1064 nm (9398 cm^{-1}) with power up to 2.5 W using an InGaAs-detector. For measuring Raman spectra, a DXR spectrometer (Thermo-Nicolet, USA) was used with laser excitation at λ = 780 nm, with a diffraction grating of 1800/mm, slit widths of 25 and 50 μm and spectral resolution of 2–5 cm^{-1}. For remote measurements, a 5-m fiber optic cable with a retro-scattering probe model RPL780/12-5 with a focal length of 5 mm and a numerical aperture of 0.4 was used. The total measurement times were less than 5 min for Raman spectra and about 20 min for FT Raman spectra.

The structural band of C=C stretching vibrations with two low-frequency shoulders in the range of 1710–1610 cm^{-1} is deconvoluted into three components, the structural band of $CH_{2,3}$ bending vibrations — into four components. First, linearization and subtraction of the baseline were performed. The Raman spectra are approximated by convolution of the Gauss and Lorentz functions. Component bands parameters were fitted using optimization programs included in the Omnic application package for the Thermo-Nicolet spectrometer, USA.

Results and Discussion. SLH FT, characterized by a high (up to 60 wt.%) content and diversity of olefins in a mixture of paraffins and isoparaffins, presented a difficulty in determining the total unsaturation (of the total olefins) by standard chromatographic methods (ASTM D1319, D6839, and D5134) and by the iodine number determination method (GOST 2070), which showed significant discrepancies ([3], Table 1), which was one of the reasons for developing a Raman spectroscopy method without correlation with standard methods.

Chemometric models for the first derivative of the Raman spectra based on model gravimetric calibration mixtures showed slightly better relative accuracy of about 3–4%, but, like the correlation models in the near-IR region, turned out to be unstable outside the training fractions and required correction when changing batches of raw materials. To develop a self-tuning model, digital Raman spectra of a wide range of olefins were investigated quantitatively.

In the Raman spectra of SLH FT in the region of C=C stretching vibrations (Fig. 1), the complex three-component structure of the 1690–1630 cm^{-1} band is visible and is recognizably similar to the three-component bands of oil products. The correlations of C=C vibration frequencies with the type of substitution and C=C bond position are known from [13] and are shown in the inset in Fig. 1. Spectrum 1 refers to the low-boiling fraction (lb) up to 140^{o}C (according to which the method for determining olefins was developed), spectrum 5 — to the high-boiling (hb) fraction boiling at above 140^{o}C. Spectrum 5 in the range of 1560–1390 cm^{-1} is deconvoluted into four components: 1455 cm^{-1} corresponds to δCH_3, 1466 and 1438 cm^{-1} — to the Fermi resonance doublet of the δCH_2 scissoring vibration and the $\gamma(CH_2)_n$ rocking overtone, 1418 cm^{-1} — to $\delta C^{\alpha}H_2$ in H_2C^{α}=CHR.

To quantify the total unsaturation from the Raman spectra, concentration calibration of the ratio of the total integrated intensity of the complex C=C vibrations band in the range of 1690–1630 cm^{-1} to the integrated intensity of the $CH_{2,3}$ bending

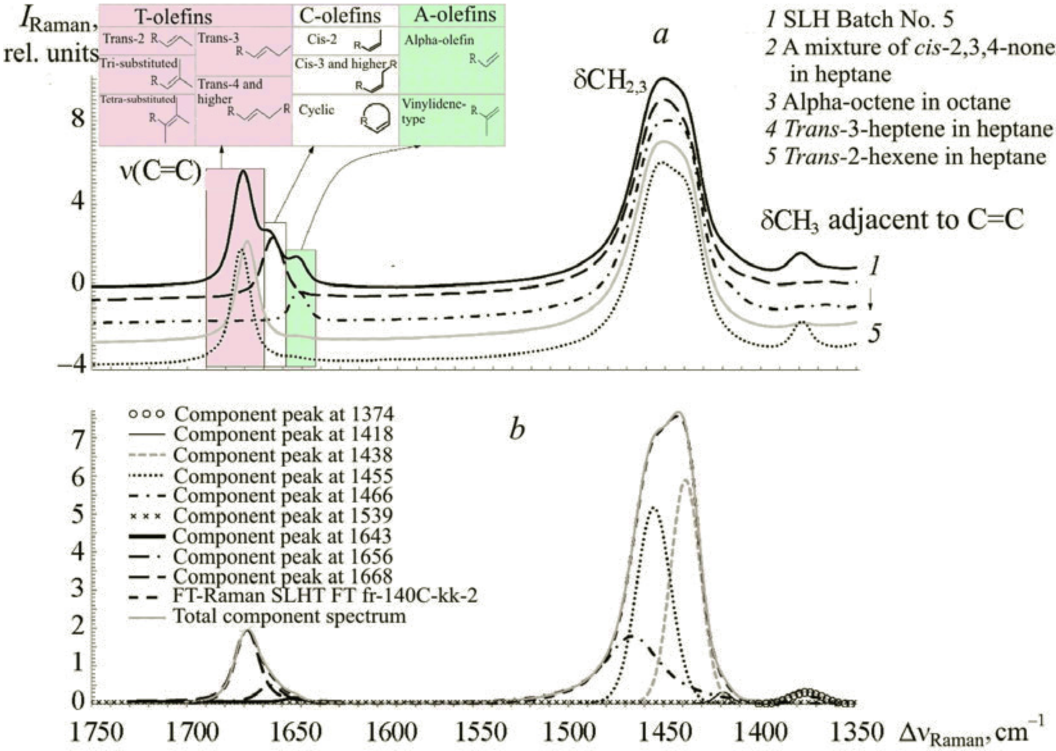

Fig. 1. Raman spectra of SLH FT (lb-140^{o}C fraction) and model mixtures of A-, C-, T-olefins in paraffins, which approximate the Raman spectra of SLH FT (a); T-olefins — a high-frequency group (*trans*-configuration in the second and higher positions from the beginning of the chain, tri-, tetra-substituted and other olefins); C-olefins — mid-frequency group (*cis*- and cyclic olefins with C > 5); A-olefins — low-frequency group (α-olefins, terminal unsaturation and vinylidene-type unsaturation); b — deconvolution of the SLH FT spectrum of the 140^{o}C-hb fraction into components.

TABLE 1. Data from Various Methods for Analyzing the Olefin Fraction (wt.%) in SLH FT No. 5

ASTM D 5134	GC, normalization method	ASTM D1319	GOST 2070	Hydrogenation/GC (Pd/C Catalyst)
36.8	37.6	59.7	17.1	47.8

vibrations band at ~1440 cm^{-1} or CH$_2$ twisting vibrations band at ~1300 cm^{-1} is required (the first one is preferable as a conditional internal intensity standard for SLH FT due to the integration of signals from all hydrocarbons, certainty of the baseline and greater intensity). Total integration of the contour without taking into account the differences in the scattering cross-sections of the C=C-stretching bands of the terminal and internal unsaturated groups, which are observed with a variation in the ratios of the components, leads to a significant scatter of the results. Therefore, it is advisable to deconvolute the complex peak into three components and calibrate for each separately. The ratio of the intensities of Raman bands of C=C vibrations (I_{CC}), reduced to the intensities of the Raman bands of the CH bending vibrations (I_{CH}) of one C atom, for model olefins with internal unsaturation and terminal unsaturation (α-olefins) differs on average ~1.36 times (Fig. 2). Consequently, the determination of total unsaturation from extrapolation of a calibration built based on an A-olefin monomer band to the total area of all C=C vibrations (for example, by adding the A-olefin to SLH FT or by controlling the polymerization using known quantitative monomer feed) can lead to deviations of as much as 30% and more. Another source of errors can be differences in the spectral properties of olefins with unsaturation in the second position (β-olefins). Analysis of Fig. 2 shows that the reduced intensities of Raman bands of T- and C-group olefins with internal unsaturation significantly differ from the average

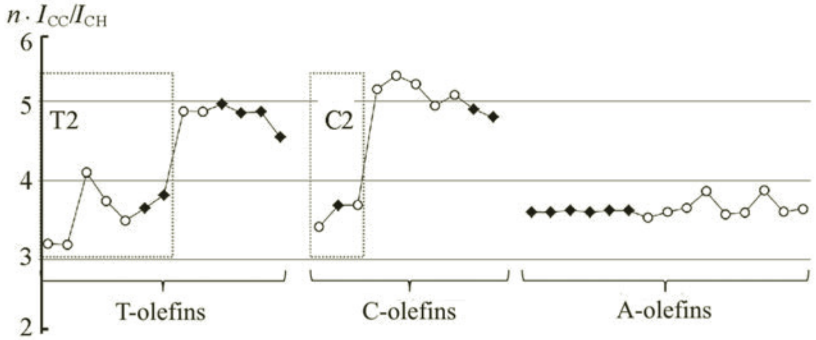

Fig. 2. The ratio of the intensity of the Raman band of C=C stretching vibrations to the intensity of the $CH_{2,3}$ bending vibrations band for *n* carbon atoms, reduced to one carbon atom (with the exception of quaternary C atoms without CH bonds in tri- and tetrasubstituted C=C), for various olefins; data from the digital collection of Raman-spectra (o); samples used for calibration solutions (♦).

values corresponding to terminal unsaturation of A-group olefins, and at a fixed C=C bond position in a homologous series up to C18 are almost invariant to the length of the aliphatic chain, which is well marked in a series of α-olefins. For A-group olefins, the dependence of the intensity ratio of $\delta CH_{2,3}$ reference bands at ~1440 cm^{-1} to the intensities of ν(C=C) bands on the number of carbon atoms in the range up to C18 is linear with high accuracy of approximation $R^2 = 0.9995$. This agrees with previous data [14, 15], where changes in the spectral characteristics of various bands relative to the intensity of the band at ~1300 cm^{-1} are monotonic with changing $1/n$ in the homologous series of paraffins and change abruptly with the number of C atoms above 17. At the same time, when the C=C bond shifts from the first to the second position, its intensity practically does not increase, and from the second to the third position it increases very noticeably; while in the fourth position (possibly higher[*]) the additional increase is rather small. A more adequate SLH representation of the reduced intensities (Fig. 2) is possible in a model mixture of olefin with paraffin, but since half of the olefins were available only in the form of spectra stored on magnetic carriers, the reduced intensities were compared using spectra of individual olefins.

The unsaturation in the β-position has hybrid spectral properties, as in the group of tri- and tetrasubstituted olefins: in terms of the reduced intensity, the ν(C=C) bands are weaker than the internal ones and are similar to group A, but in frequency they resemble the internal bonds of the T or C groups according to their stereoisomerism. The tri- and tetrasubstituted olefins in group C were investigated as cyclic compounds with the >5 carbon atoms. The strong overlapping of the bands inside the T group does not allow one to isolate β-, tri-, and tetrasubstituted olefins (hereafter, the T_2-olefins group) by deconvoluting overlapping contours. However, the presence of an additional spectral feature allows one to take into account the T_2-olefin fraction and to quantify the decrease in the total intensity of the bands of internal unsaturation. This additional feature of T_2 olefins is that the intensity of the 1380 cm^{-1} band corresponding to CH_3 bending vibrations at the C=C bond is significantly higher than is usual for this band of asymmetric bending vibrations of aliphatic CH_3 groups, which are not very active in Raman spectroscopy, which is used for autocorrection of calibration graphs (self-tuning model feedback). A small magnitude of the base for counting the increase in the intensity of the 1380 cm^{-1} band in the absence of CH_3–CH=CH–R was determined from the spectra of hydrogenated SLH FT and paraffins–isoparaffins mixtures adequate in terms of the CH_3/CH_2 ratio.

In addition, β-*cis*-, β-*trans*-, tri-, and tetrasubstituted olefins differ from other *cis*- and *trans*-olefins with internal unsaturation in the third and higher positions by a slightly higher frequency, but the maximum of the C=C stretching vibration is spectrally unresolvable, which is clearly visible in the bands of the T-group (Fig. 1). Due to the significantly lower content of *cis*-unsaturation compared with the generally energy-preferred *trans*-unsaturation, the β-*cis*-fraction in other *cis*-olefins was not determined from the ~1370 cm^{-1} band (when separated from the 1380 cm^{-1} component by deconvolution) due to an insignificant increase in accuracy with respect to the increasing complexity of procedures. Instead, equimolar calibration mixtures of β-*cis*- with *cis*-3- and *cis*-4-olefins in paraffins were prepared.

---

[*] The ratios of reduced Raman intensities measured from digital Raman spectra [10] in *cis*- and *trans*-polyoctenamers (with one double bond per eight CH_2 groups) turned out to be close to the values for octenes with internal unsaturation.

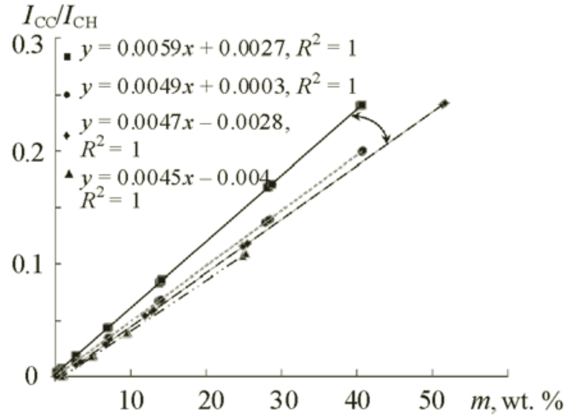

Fig. 3. Dependencies of intensity ratios I_{CC}/I_{CH} on mass fraction *m* of paraffin solutions of *trans*-3- (■), *trans*-2-olefins (♦), 1-octene (▲) and mixtures of 2-, 3- and 4-*cis*-nonenes (●).

Deconvolution of the complex spectrum of the ν(C=C) band into three components by the convolution of the Gauss and Lorentz functions (Fig. 1) yields a good approximation with a relative standard deviation of <0.1% of the total area. The three components obtained by the spectral deconvolution of C=C stretching vibrations in SLH FT spectra are compared with the ν(C=C) bands of Raman spectra of individual model olefins and their paraffin solutions. The half widths of the C-, T-, and A-components of the SLH FT deconvolution exceed the half widths of C=C vibrations of the individual *cis*-, *trans*-, and α-olefins. The deconvolution components corresponding to the C- and T-forms are well described in half-width by the corresponding binary mixtures of (*cis*-2 + *cis*-3)- and (*trans*-2 + *trans*-3)-olefins.

It has been established that to compile minimally complex model mixtures that are adequate in spectral properties of SLH FT, it is necessary to choose five types of olefins corresponding in mass to the average fraction and having an unsaturation in the first position, a *cis*- and *trans*- unsaturation in the second, third or higher positions.

The high intensity of CH_3 bending vibration bands at the C=C bond makes it possible to estimate the fraction of T_2-olefins in the T-component of deconvolution using the ratio for the fraction of β-olefins (P_2):

$$P_2 = \frac{\left(i_{1380}^{\max(\mathrm{SLH})} - I_{1380}^{\max(trans\text{-}3)}\right)\Big/\left(i_{1670}^{\max(\mathrm{SLH})} - I_{1670}^{\max(trans\text{-}3)}\right)}{\left(I_{1380}^{\max(trans\text{-}2)} - I_{1380}^{\max(trans\text{-}3)}\right)\Big/\left(i_{1670}^{\max(trans\text{-}2)} - I_{1670}^{\max(trans\text{-}3)}\right)}, \tag{1}$$

where max $I_{1380}^{\max}$ and $I_{1670}^{\max}$ are the maximum intensities of the peaks at ~1380 and ~1670 cm^{-1}; and $i_{1380}^{\max}$ is the peak maximum intensity corrected for the baseline contribution of paraffin CH_3 groups not associated with the unsaturated group.

To calculate the "pure" contribution of δCH_{1380} of CH_3 groups conjugated with the C=C bond, it is necessary to determine the base contribution of asymmetric δCH of paraffinic CH_3 groups from the Raman spectrum of fully hydrogenated SLH FT. The subtracted contribution at 1380 cm^{-1} is normalized to the $\delta CH_{2,3}$ bands at ~1450 cm^{-1} and is determined from the expression:

$$i_{1380}^{\max} = \left[\frac{I_{1380}^{\max(\mathrm{SLH})} - I_{1380}^{\max(\mathrm{hydr.SLH})}}{I_{1450}^{\max(\mathrm{SLH})} - I_{1450}^{\max(\mathrm{hydr.SLH})}}\right] I_{1450}^{\max(\mathrm{SLH})}. \tag{2}$$

The ratios of the T_2-fraction in LHC of various batches and fractions thus estimated show a fairly wide variation in their content with P_2 fluctuations in the range of 0.2–0.7. The P_2 variation is accompanied not only by an increase in the relative intensity of the 1380 cm^{-1} band, but also by a correlated high-frequency shift of the ν(C=C) band maximum from 1670 to 1673 cm^{-1}.

Samples of olefins, whose histograms are shown in Fig. 2, were used to prepare four sets of calibration solutions in paraffins in a wide range of concentrations. Both, mass percentages and the number of C=C bonds per 100 carbon atoms were used as the concentration units in the developed laboratory procedure. These units can be easily converted to mass, volume percent and iodine value. The advantage of such units of measurement is the universality of the calibration in C=C/100C, applicable to different LHC fractions, since it eliminates the need to construct separate calibration curves for fractions with different boiling points (chain lengths). Traditional calibrations performed in mass percent for a specific fraction cannot be directly used for another fraction, which is a typical disadvantage of chemometric models based on near-IR spectra.

Figure 3 shows the calibration dependences of the intensity ratio of the bands ν(C=C)/δ$CH_{2.3}$ on the concentration of *trans*-2-olefins (as the average characteristic of the T_2-group), *trans*-3-olefins (hereinafter T_3), mixtures of (*cis*-2 + *cis*-3 + *cis*-4)-olefins and α-olefins in various paraffins, as well as mass percentages for comparison with data obtained by other methods.

The self-tuning algorithm for calculating the total olefins content ($Y = Y_A + Y_C + Y_T$) using calibration mixtures of four different types of olefins (A, C, T_2, T_3) in the form of three spectrally resolvable components is quite simple. After collecting the Raman spectrum of LHC TF, the integrated intensities of the C=C stretching (I_{CC}, 1710–1610 cm^{-1}) and $CH_{2,3}$ bending vibration bands (I_{CH}, 1560–1390 cm^{-1}) are used to calculate I_{CC}/I_{CH}. Further, the contour of the C=C-stretching vibration band is deconvoluted into components A + C + T, the percent contribution of the areas S_A, S_C, S_T of each component to the total area of the band ν(C=C) is determined, as well as the arguments $X_{A,C,T} = (S_{A,C,T}/100)\ (I_{CC}/I_{CH})$ for model calibrations. From the calibration equations of the form $Y = kX$ (for convenience of comparison, Figs. 2 and 3 show the inverse dependences of the relative intensities y on the concentration x), the content of A- and C-olefins is determined. To correctly determine the T-group, the coefficient P_2 is used and the content of T-olefins is calculated

$$Y_T = (k_{T3} + P_2(k_{T2} - k_{T3}))X_T\,.$$

Units of measurement can be either traditional in the form of olefin concentrations, or characterizing the degree of unsaturation (C=C/100C). In the latter case, they can be easily transformed to iodine values, and can also be used for different fractions of hydrocarbons with the number of atoms C <18. The intensity ratios νCH_3/νCH_2 in all fractions up to 140°C varied less (<8%) than when compared with high-boiling fractions. Above C18 in calibrations, one should take into account the decrease in the proportion of isoparaffins, the spectral changes of the Fermi-resonant doublet of the scissoring and IR-active overtone of the CH_2 twisting vibrations (2 × 720 cm^{-1}) in the contour of the $CH_{2,3}$ bending vibrations due to aggregate changes in intermolecular interactions.

Eleven batches of SLH FT were measured with measurements repeated three to eight times at different times for each batch. The results were compared using the accuracy indicators of the method of multidimensional gas chromatography according to ASTM D6835 (Reformulyzer, Table 2). According to Student's test,

$$t_m = |\theta_m| \Big/ \sqrt{S^2_{c,m}\big/L + \Delta^2_{0,m}\big/3.8}\,, \tag{3}$$

(θ_m is the divergence of X_m measurement results obtained by different methods; $S_{c,m}$ is the RMS of the results of two compared methods; $S_{r,m}$ is the error characteristic of the test method; $\Delta_{0,m}$ is the determined error characteristic of the analysis results by the comparison method) t_m must be smaller than t_{tabl} (with $f = 2$–7, $P = 0.95$) [16].

The average divergence $|\theta_m| = 0.99$. The data in Table 2 indicate absence of statistically significant differences between the two methods. The standard deviation of repeatability for seven batches of LHC FT ($W = 7$) measured on a Fourier transform spectrometer (S_r or S_R)** is found by:

$$S_r = \sqrt{\frac{1}{W}\sum_{w=1}^{w}\frac{\sum_{i=1}^{N'}(X_{w,i} - X_{w,i})^2}{N' - 1}} = 0.74 \text{ wt.\%}\,. \tag{4}$$

The relative standard error of measurements of the total olefin content in the range of 40–60 wt.% by the Raman spectroscopy method is ≤1.5% (the accuracy of Raman is slightly higher than of ASTM D6835). Along with the initial batches, residual olefins in the processes of hydrogenation and hydroformylation were analyzed. Relative error of Raman measurements, % (in the middle of the range, wt.%): ~5 (2.5–10), ~2.5 (10–40) and ~1.5 (40–60); the relative error according to ASTM D 5134: ~8 (1–10) and ~5 (10–40). Relative error according to ASTM D 1319, % (for the specified content of olefins, vol.%): ~10 (15), ~8 (20), ~7.2 (25). Convergence in the standard method for determining the iodine number of light petroleum products according to GOST 2070-82 (methods A and B) at the same laboratory on the same oil product sample does not

---

[**] This accuracy was obtained with a 2003 Fourier Raman spectrometer, and on a modern DXR Raman spectrometer the precision of single measurements is much higher.

TABLE 2. Total Olefins in SLH FT According to Raman Data and ASTMD6835

Sample	Raman		Reformulyzer M3		Divergence $|\theta_m|$	$t_m^{\max}$	t_{tabl} ($f = 2–7$, $P = 0.95$)	Correctness ($t_m < t_{\text{tabl}}$)
	X_m	$S_{r,m}$	X_m	$\Delta_{0,m}$				
Batch No. 5	55.68	0.49	56.08	0.83	0.40	0.78	2.37	+
Batch No. 5Na	56.13	0.78	56.32	0.83	0.19	0.34	2.37	+
Batch No. 6	50.73	1.34	52.26	0.80	1.53	2.23	2.45	+
Batch No. 7	52.23	1.17	52.42	0.80	0.19	0.30	2.37	+
Batch No. 7Na	51.43	0.78	53.12	0.81	1.69	2.29	2.37	+
Batch No. 8	58.01	0.50	55.98	0.83	2.03	2.87	3.18	+
Batch No. 9	50.82	1.06	–	0.79	–	–	–	–
Batch No. 10	49.62	0.47	50.52	0.83	0.90	1.84	4.30	+

exceed 10% of the lower result by method A and 15% by method B. At present, ASTM WK34260 is being tested on the application of Raman spectroscopy for the determination of olefins in gasolines: when the olefins content is 7%, the absolute accuracy of the method is 0.5%, and at 25% – 1.0% [17].

Therefore, our proposed method [18] for the determination of olefins using Raman spectroscopy exceeds the existing methods for the analysis of olefins in accuracy.

Conclusions. The developed method allows to determine the three main types of olefins and the fraction of *trans*-β-, tri- and tetrasubstituted olefins in the group of T-olefins, as well as total olefins with a relative error of ~5% in the middle of the 2.5–10 wt.% range, ~2.5% in the middle of the 10–40 wt.% range, and ~1.5% in the middle of the 40–60 wt.% range. Self-tuning of the model by calculating the proportion of spectrally unresolvable C=C components from the intensity of conjugated methyl groups increased its accuracy. In terms of repeatability for one laboratory, the accuracy of the method exceeds the standard methods (ASTM D1319, D6839, D5134, GOST 2070). To calibrate the method, five types of model solutions of olefins in paraffins are sufficient. The C=C/100C units of measurement allow to convert the data into iodine numbers and unify the calibration model for different fractions, regardless of the mass (chain length) of hydrocarbons. The accuracy and reliability of the method is confirmed by parallel comparison of data with a known method. The method allows both to carry out measurements in the laboratory and remotely control processes and product pipelines through fiber optic cables.

REFERENCES

1. P. Chabot, M. Simpson, and F. Melas, *Special Report, Instrumentation & Analytics. ABB Review*, 54–60 (2006).
2. Strategies for Achieving Optimal Gasoline Blending; https://www.honeywellprocess.com/library/marketing/casestudies/WhitePaper_Valero_OptimizedGasolineBlending.pdf (accessed December 27, 2018).
3. A. Kh. Kuptsov, O. G. Karchevskaya, E. E. Kron, and E. V. Zhmaeva, *Neft. Khoz.*, No. 10, 125–127 (2016).
4. D. L. Gerrard, In: *Analytical Raman Spectroscopy Chemical Analysis*, **114**, Eds. J. G. Grasselli, B. J. Bulkin, Ch. 9, John Wiley & Sons Inc., New York (1991).
5. A. L. Lapidus and O. L. Eliseev, *Gazokhimiya*, No. 1, 26–30 (2008).
6. X. Zhang, X. Qi, M. Zou, and J. Wu, *J. Raman Spectrosc.*, **43**, No. 10, 1487–1491 (2012).
7. K. M. Tan, I. Barman, N. C. Dingari, G. P. Singh, T. F. Chia, and W. L. Tok, *Anal. Chem.*, **85**, No. 3, 1846–1851 (2013).
8. Rory H. Uibel, Robert E. Benner, Eric R. Jacobsen, and Lee M. Smith, *Methods for Determining Olefin Concentrations in Olefin-Containing Fuels*, US Patent No. 7973926 B1 (2011).
9. J. A. Ardila, F. L. F. Soares, M. A. S. Farias, and R. L. Carneiro, *Anal. Lett.*, **50**, No. 7, 1126–1138 (2017).
10. A. H. Kuptsov and G. N. Zhizhin, *Handbook of Fourier Transform Raman and Infrared Spectra of Polymers*, Elsevier Science, Amsterdam (1998), p. 581.
11. Elsevier FT-Raman and FT-IR Polymer Database for ACD/Labs; https://www.acdlabs.com/products/dbs/ir_raman_db/ (accessed December 27, 2018).
12. A. Kh. Kuptsov and G. N. Zhizhin, *Fourier Transform Raman and Fourier Transform IR Spectra of Polymers* [in Russian], Tekhnosfera, Moscow (2013).

13. G. Socrates, *Infrared and Raman Characteristic Group Frequencies. Tables and Charts*, 3rd ed., John Wiley & Sons Ltd. (2001), pp. 68–78.
14. Yu. V. Shemuratov, E. A. Sagitova, K. A. Prokhorov, G. Yu. Nikolaeva, and P. P. Pashinin, in: *Coll. Sci. Works "Physical Chemistry of Polymers. Synthesis, Properties and Application"* [in Russian], Tver State University, Tver, Vol. 15 (2009), pp. 51–62.
15. Yu. V. Shemouratov, K. A. Prokhorov, G. Yu. Nikolaeva, P. P. Pashinin, A. A. Kovalchuk, A. N. Klyamkina, P. M. Nedorezova, K. V. Demidenok, Yu. A. Lebedev, and E. M. Antipov, *Laser Phys.*, **18**, No. 5, 554–567 (2008).
16. RMG 61-2010 State system for ensuring the uniformity of measurements. Indicators of accuracy and precision of methods for quantitative chemical analysis. Evaluation methods [in Russian].
17. Raman Method Improves Olefin Measurement. Process Instruments Inc., https://www.rdmag.com/product-release/2009/03/raman-method-improves-olefin-measurement (accessed July 20, 2016).
18. A. Kh. Kuptsov, T. E. Kron, O. G. Karchevskaya, and G. A. Korneeva, *"Method for the Determination of Olefin in Synthetic Liquid Hydrocarbons Obtained by the Fischer–Tropsch Method (Versions)"* [in Russian], RF Patent No. 2581191 (2016).